

General Disclaimer

One or more of the Following Statements may affect this Document

- This document has been reproduced from the best copy furnished by the organizational source. It is being released in the interest of making available as much information as possible.
- This document may contain data, which exceeds the sheet parameters. It was furnished in this condition by the organizational source and is the best copy available.
- This document may contain tone-on-tone or color graphs, charts and/or pictures, which have been reproduced in black and white.
- This document is paginated as submitted by the original source.
- Portions of this document are not fully legible due to the historical nature of some of the material. However, it is the best reproduction available from the original submission.

N.I.

SQT

OLD DOMINION UNIVERSITY RESEARCH FOUNDATION

DEPARTMENT OF MECHANICAL ENGINEERING AND MECHANICS
SCHOOL OF ENGINEERING
OLD DOMINION UNIVERSITY
NORFOLK, VIRGINIA

EXPERIMENT AND ANALYSIS ON THE FLOW PROCESS
DYNAMICS OF THE NASA-LANGLEY EIGHT-FOOT
TRANSONIC PRESSURE TUNNEL

(NASA-CR-154806) EXPERIMENT AND ANALYSIS ON THE FLOW PROCESS DYNAMICS OF THE NASA-LANGLEY EIGHT FOOT TRANSONIC PRESSURE TUNNEL Semiannual Progress Report, 1 May 1976 - 28 Feb. (Old Dominion Univ. Research

N77-30085

HC A03/MF A01

Unclas

G3/02 42120



By

Ping Tcheng

Semiannual Progress Report

Prepared for the
National Aeronautics and Space Administration
Langley Research Center
Hampton, Virginia

Under
NASA Grant NSG 1079
May 1, 1976 - February 28, 1977
John S. Tripp, Technical Monitor
Instrument Research Division

August 1977



DEPARTMENT OF MECHANICAL ENGINEERING AND MECHANICS
SCHOOL OF ENGINEERING
OLD DOMINION UNIVERSITY
NORFOLK, VIRGINIA

EXPERIMENT AND ANALYSIS ON THE FLOW PROCESS
DYNAMICS OF THE NASA-LANGLEY EIGHT-FOOT
TRANSONIC PRESSURE TUNNEL

By

Ping Tcheng

Semiannual Progress Report

Prepared for the
National Aeronautics and Space Administration
Langley Research Center
Hampton, Virginia

Under
NASA Grant NSG 1079
May 1, 1976 - February 28, 1977
John S. Tripp, Technical Monitor
Instrument Research Division



Submitted by the
Old Dominion University Research Foundation
Norfolk, Virginia 23508

August 1977

DEPARTMENT OF MECHANICAL ENGINEERING AND MECHANICS
SCHOOL OF ENGINEERING
OLD DOMINION UNIVERSITY
NORFOLK, VIRGINIA

EXPERIMENT AND ANALYSIS ON THE FLOW PROCESS
DYNAMICS OF THE NASA-LANGLEY EIGHT-FOOT
TRANSONIC PRESSURE TUNNEL

By

Ping Tcheng

Semiannual Progress Report

Prepared for the
National Aeronautics and Space Administration
Langley Research Center
Hampton, Virginia

Under
NASA Grant NSG 1079
May 1, 1976 - February 28, 1977
John S. Tripp, Technical Monitor
Instrument Research Division



Submitted by the
Old Dominion University Research Foundation
Norfolk, Virginia 23508

August 1977

EXPERIMENT AND ANALYSIS ON THE FLOW PROCESS DYNAMICS OF THE
NASA-LANGLEY EIGHT-FOOT TRANSONIC PRESSURE TUNNEL

By

Ping Tcheng¹

INTRODUCTION

This report describes a dynamic response test performed at the NASA-Langley eight-foot transonic pressure tunnel. The objective of the test is to obtain the dynamics of the flow process of this wind tunnel at transonic conditions. It is contemplated that the test results will provide not only a better understanding of the transient behavior of the flow process but also a means for substantiating the mathematical modeling effort currently being developed for the National Transonic Facility. Included in this report are descriptions of the test conditions, instrumentation, presentation of raw data, analysis of data, and finally, based on experimental evidences, an attempt to construct an input-output relationship of the flow process from the viewpoints of control engineering.

TEST DESCRIPTION

The dynamic response of the flow was measured as disturbances were introduced into the flow. Disturbance in the form of drag-force change was initiated in the test section as an input signal to perturbate the equilibrium of the flow process around the wind tunnel circuit. Measurements were made on the source of disturbance in the test section and on the response or perturbations generated by the disturbance at various locations around the wind tunnel circuit. Pertinent information on the test is listed below.

¹ Associate Professor, Department of Mechanical Engineering and Mechanics, Old Dominion University, Norfolk, Virginia 23508.

Test Parameters

The wind tunnel condition was set with the following envelope:

Mach number - .4, .6, .8, 0.95, 1.05, 1.2

Total pressure - one atmosphere

Fan power - constant

Temperature - stagnation station (big end) controlled at 49° C (120°F)

Test Models

Two models were used for providing disturbances in the test section:

1. Flap model - 40 in.² wedge, sting mounted*
2. Aero model - airplane, floor mounted

Test Inputs

Two types of inputs or sources of disturbances were generated:

1. Static input (step input)
 - a. Flap model - stepwise opening or closing
 - b. Aero model - stepwise changing of angle of attack
2. Dynamic input (periodic input at 0.1 Hz)**
 - a. Flap model - periodical opening or closing
 - b. Aero model - periodical changing of angle of attack

* Different sizes of flaps were fabricated but not tested.

** These periodical signals are square waves. Signals with frequencies higher than 0.1 Hz were applied unsuccessfully due to the power limitation of the driving mechanism.

Instrumentation

A large number of measurements on the pressures, temperatures, power, etc. at different sites of the wind tunnel circuit were made using various kinds of instruments and transducers. Shown in figure 1 is an instrumentation schematic indicating the types and locations (referenced by three-digit station numbers) of measurements made. Figure 2 shows a detailed instrumentation schematic in the test section for the flap model test. Two precision manometers, one for monitoring the stagnation pressure at station 100 and the other for the static pressure in the plenum or station 300 were also used. The manometers, their tubings and several pressure transducers are sketched in figure 3. The manometer outputs along with all the temperature measurements were recorded in digital forms on the SEL system. The sampling periods on the SEL are one second for static input tests and two seconds for dynamic input tests. All other measurements were recorded in analog forms on two 13-channel FM tape recorders. FM tapes were played back and recorded on a multichannel oscillograph after the test for analysis. As for the sources of disturbances, the drag force exerted on the wedge was measured by a single-component balance, and the angle of attack was measured by a potentiometer. These two signals were recorded on the SEL system and on the FM tape recorder.

GENERAL REMARKS ON THE TEST RESULTS

It is now appropriate to make several remarks on the results of the test since they are relevant to the data presentation and system analysis to be discussed in later parts of this report. Remarks on the quality of the test results as related to the test models, test inputs and instrumentation will be first made separately and then followed by a summarized statement.

Test Models

1. Flap model - smooth signals obtained
2. Aero model - scattered signals obtained and considered useless for analysis

Test Inputs

1. Static input - excellent step function generated
2. Dynamic input - excellent square wave function generated at 0.1 Hz only

Instrumentation

1. Drag force - excellent balance output recorded
2. Temperatures - temperature variation less than $\pm 2^\circ$ F, variations within error band of the thermocouples used, variations considered insignificant and useless
3. Fan Power - AC motor current excellently recorded, no variation detected
4. Total pressures (FM) - good quality signals from strain gage pressure transducers, hardcopy records from oscillograph of 10 percent accuracy
5. Static Pressures (FM) - Very small variations of static pressures recorded, only qualitative but not quantitative information obtained*
6. Total pressure (SEL) - accurate total pressure at station 100 (big end) recorded from manometer
7. Static pressure (SEL) - accurate static pressure at station 300 (plenum) recorder from manometer

Thus, it can be seen just a small portion of the test results is available and useful for data reduction purposes. For this reason, only data obtained from the flap model test will be presented. The system analysis will include two parts: a qualitative analysis from the FM records and a limited quantitative one from the SEL data.

* Atmospheric pressure was inadvertently used as the reference for static pressure measurements. Even though the full scale values of transducers were selected correctly, variations in static pressures (AC variations) were found to be not more than 8 percent of the nominal static pressures (DC references).

DATA PRESENTATION

Data of 20 static tests and 7 dynamic tests using the flap model with nominal Mach number settings ranging from 0.80 to 1.20 are presented in this section. Since it is impractical and unnecessary to include the entire amount of data collected in this report, results of test run no. 19 are selected for illustrated presentation. Run 19.31, a typical static test which illustrates the transient response characteristics of the flow process is presented first and followed by the dynamic test of run 19.35. A brief description and characterization of the results are included.

Run 19.31 (Static test)

The nominal mach number setting was 1.05. The actual Mach number prior to the test run was found at 1.053 with the flap closed. The flap was suddenly opened at the start of the run. The run lasted about 40 seconds until a new equilibrium condition in the wind tunnel circuit was reached. The final mach number was .980.

SEL data recorded at the start (state 1) and the end (state 2) of this run provided the following information:

$$\text{Drag force: } D_1 = 259 \text{ lb}_f$$

$$D_2 = 455 \text{ lb}_f$$

$$\Delta D \equiv D_2 - D_1 = 196 \text{ lb}_f$$

$$\text{Total pressure: } P_{t1} = 14.72 \text{ psi}$$

$$P_{t2} = 14.55 \text{ psi}$$

$$\Delta P_t \equiv P_{t2} - P_{t1} = -.17 \text{ psi}$$

$$\text{Static pressure: } P_{s1} = 7.30 \text{ psi}$$

$$P_{s2} = 7.87 \text{ psi}$$

$$\Delta P_s \equiv P_{s2} - P_{s1} = .57 \text{ psi}$$

Mach number*: $M_1 = 1.053$

$M_2 = .980$

$\Delta M \equiv M_2 - M_1 = .073$

The following qualitative observation is made from the SEL data: As more load is introduced into the test section, which is evidenced by an increment in drag force ($\Delta D > 0$), the mach number is decreased ($\Delta M < 0$), the static pressure is increased ($\Delta P_s > 0$) and the total pressure is decreased ($\Delta P_t < 0$). The opposing changes of the two pressures, that is, when one is increased then the other is decreased and vice versa, have been observed in all other runs. Percentage changes of these two pressures as well as their relative contribution to the Mach number change will be discussed in System Analysis.

Test results of run 19.31 are presented from figures 4 through 13:

Drag force.-Figure 4 shows the step increase of the drag force exerted on the flap as it is opened from the closed position. Both FM and SEL recordings are shown. The FM trace signal resembles very much a step input. The SEL signal, on the other hand, clearly indicates a finite rise time which is believed to be caused by the filter used on the SEL system.

101T.-Figure 5 shows the transient response of the total pressure measured by transduced 101T located at the big end. The SEL recording of the total pressure measured by the manometer is also included for comparison. This first-order response with a time constant on the order of 8 seconds is observed. It is noticed that the SEL system is capable of reproducing the slow varying total pressure change in this case. Transport lag or dead time T_d between this response and the drag force trace shown in figure 4 is not recognizable. The existence of the transport lag, however, plays an important role in the analysis of the dynamic test results. Based on this reasoning and for the simple fact that all distributed parameter processes, such as the wind tunnel flow process on hand, do possess finite transport lag, it is concluded that a small T_d of one second or less might exist between the big end and the test section of the wind tunnel.

201S.-Figure 6 shows the static pressure change in the test section measured by a wall-mounted transducer (201S) located 6.5 inches upstream

* The Mach number computation was based on pressures listed above.

of the flap. Though the signal level is rather small, a sharp step change or sudden increase in static pressure is clearly observed as soon as the flap is opened. Contrary to the two signals mentioned above, this signal does not have a counterpart measured on the SEL system. The manometer and SEL system will not be able to reproduce this fast changing pressure in any case.

201T.-Figure 7 shows the total pressure change in the test section measured by transducer 201T. The trace shown here resembles that of figure 5 (101T) with the exception that the former should have a smaller transport lag since 201T is located closer to the flap.

701T.-This transducer is located two corners downstream from the test section. Figure 8 shows the total pressure change measured at that corner. Other than the trace being a bit noisy caused by the turbulence generated by the fan located just upstream of station 700, it again resembles the one shown in figure 5.

401T, 801T, 901T.-Total pressures measured at the other corners of the wind tunnel circuit by these transducers are not shown since they all resemble the total pressure measured by 101T.

701S.-Transducer 701S which is located adjacent to 701T measures the static pressure at station 700. The trace from it is shown in figure 9. The trace from this figure is almost identical to the one shown in figure 8 (701T) if the noise contained in the latter is removed. In other words, the total pressure is equal to the static pressure at all times due to low flow velocity at station 700.

401S, 801S, 901S.-The remarks made on the response from 701S with respect to the response from its counterpart 701T also apply to these static pressure measurements as compared to their respective counterparts. Responses from these transducers are not presented.

301S, 302S.-These two transducers measure the static pressure in the plenum at two different sites. Measurements made by transducer 302S is shown in figure 10. It is suggested that first-order type response illustrated is resulted from the dynamics of filling the plenum through the slotted openings between the plenum and the test section as the pressure of the latter is suddenly increased. The time constant calculated is approximately four seconds, which is smaller than the magnitude demonstrated in the total

pressures measured around the wind tunnel circuit. This figure also includes the SEL recording from an ideal manometer which has its probe located in the plenum. The FM and SEL recordings do not seem to resemble each other. The slow SEL recording is believed due to the dynamics of the manometer. Since the plenum and test section have identical static pressures under steady-state or equilibrium conditions, the SEL recording can be used as an accurate measure of the steady-state static pressure in the test section. Similiar response from 301S was observed and therefore not presented.

HO.--This transducer measures the same total pressure fed to the ideal manometer located in the control room (see figure 3). The recording from HO and the one from 101T are found identical. Since the two transducers are separated by more than 200 feet of metal tubing, it is noticed that tubing dynamics is negligible in this case. Measurements made by HO are not presented here.

PTCO.--Similiar to the function of transducer HO, PTCO measures the plenum static pressure approximately 100 feet downstream from the plenum. No essential difference is found between responses of PTCO and 301S. This implies that tubing dynamics can be ignored, too. Records from PTCO are not presented.

203S, 204S.--These two transducers measure the static pressures in the test section upstream from the flap (see figure 2). Measurements made are shown in figures 11 and 12. The step change in static pressure observed by 201S near the flap has been disintegrated into a waveform resembling that of 101T.

202S.--This wall-mounted static pressure transducer is located behind the flap (see figure 2). The static pressure recorded is shown in figure 13. The transient behavior is very different from the other test section measurements. It shows a sharp drop in static pressure initially, holds it for 10 seconds, and then slowly increases as a first-order system response to a final value greater than the initial static pressure.

Run 19.35 (Dynamic test)

This is the follow-up test of the static run 19.31. The nominal Mach number was set at 1.05 prior to the run with the flap in the closed position.

The flap was then alternately opened and closed at five-second intervals. Thus, the drag force input to the wind tunnel circuit is a square wave with a frequency of 0.1 Hz (0.6283 rad/sec).

SEL data of the drag force D , total pressure P_t , static pressure P_s and the computed Mach number M were analyzed using the "Fast Fourier Transform" (FFT) algorithm. Thirty consecutive samples of steady-state data recorded at two-second intervals were selected to minimize leakage. The transform contains the spectrum with a fundamental frequency at 1/60 Hz (0.1047 rad/sec) and higher harmonics at multiples of the fundamental frequency. The frequency of interest, 0.1 Hz (0.6283 rad/sec), is the sixth harmonic in the spectrum. The following results were obtained from the FFT computations:

$$\Delta D = 353.8 + 129.8 \cos (.6283t - 58.54^\circ), \text{ lb}_f$$

$$\begin{aligned} \Delta P_t &= 2106.3 + 2.802 \cos (.6283t - 169.76^\circ), \text{ psfg} \\ &= 37.4 + 2.802 \cos (.6283t - 169.76^\circ), \text{ psfa} \end{aligned}$$

$$\begin{aligned} \Delta P_s &= 1099.7 + 4.505 \cos (.6283t + 48.34^\circ), \text{ psfg} \\ &= 1044 + 4.505 \cos (.6283t + 48.34^\circ), \text{ psfa} \end{aligned}$$

$$\Delta M = 1.0101 + .0043 \cos (.6283t - 140.78^\circ)$$

The following FM recordings of run 19.35 are presented:

Drag force.-Figure 14 shows the 0.1 Hz square wave response from the balance. The record length is approximately 140 seconds.

101T.-Figure 15 shows the total pressure response measured by transducer 101T. It is observed that a steady-state sawtooth waveform was developed approximately 40 seconds after the oscillation was introduced. This amount of time required to fully develop the steady-state response is consistent with the time constant found from the static test. It should also be emphasized that the steady-state response is not sinusoidal but rather saw-toothed. As in the case of static run 19.31, all total pressure measurements, such as those of 201T, 701T, etc., resemble the total pressure measured by 101T very closely.

201S.-Figure 16 illustrates the static pressure response measured by transducer 201S. The square wave observed indicates the instantaneous nature of static pressure change in the test section.

203, 204S.-Figures 17 and 18 include the responses from transducers 203S and 204S, respectively. These measurements indicate the disappearance of the square wave pressure change near the source of disturbance as measurements are made further away from it in the test section. From records of 203S, it appears that an initial transient period is required before the steady-state waveform can be developed.

202S.-The response from transducer 202S located downstream from the source of disturbance is shown in figure 19. It illustrates that not only an initial transient period is required to fully develop the steady-state response but also that the steady-state square wave is out of phase with the square wave input shown in figure 14. The latter can be attributed to the initial transient behavior indicated in figure 13.

301S, 302S.-Pressure changes in the plenum measured by transducers 301S and 302S are shown in figure 20. The signals are small and intelligible enough to be analyzed.

This concludes the data presentation of a typical test run no. 19. With the exception of minor variations quantitatively, data obtained from other runs do not provide any additional information on the dynamics of the flow process. However, since the control of test section Mach number is of prime interest and the Mach number is determined by the total pressure and static pressure measured respectively by transducers 101T and 201S, records from these two transducers for all runs are summarized in figures 21 and 22. Time constants calculated from responses of 101T as well as from the SEL data measured by the ideal manometer are listed in table 1. The time constant of the total pressure ranges from 3.7 to 9.2 seconds. As for the static pressure change in the test section, figure 21 clearly illustrates that these changes are almost instantaneous at subsonic speed and are completed within three seconds at $M = 1.20$. Furthermore, it should be mentioned that SEL data recorded at the beginning and the end of all runs are not presented here but will be presented in the next section along with the system analysis.

Table 1. Process time constants at the big end of the wind tunnel.

Test Run	Nominal Mach No.	Average Time Constant, sec		
		SEL (#44)	FM (101T)	Eqs. (11) to (13)
19	1.05	7.7	9.2	13.5
20	1.20	3.7	5.2	3.5
21	0.95	7.1	6.7	4.5
22	0.80	5.3	5.5	4.6

SYSTEM ANALYSIS

Based on the experimental data collected, an attempt is made in this section to perform a system analysis on the cause and effect relationship of the flow process from the viewpoint of control engineering. The analysis is by no means a complete one as it is limited by the amount of quantitative information available. Steady-state SEL data will be processed first to establish gain constants, and together with the response speeds of pressure changes found in the previous section, a dynamic relationship between Mach number change and drag force change in the test section will next be constructed. Finally, a dynamic model will be constructed between the static pressure in the test section and the total pressure at the big end of the wind tunnel by analyzing the oscillating data.

Establishment of Linear Relationship Between the Mach Number and Pressures

The test section Mach number is computed from the following equation:

$$M = \sqrt{5 \left[\left(\frac{P_t}{P_s} \right)^{2/7} - 1 \right]} \quad (1)$$

where

M = test section Mach number

p_t = test section total pressure, psf

p_s = test section static pressure, psf

Equation (1) is derived quasi-statically and is applicable to equilibrium states of the wind tunnel flow. Assuming that the tunnel is initially in equilibrium state one, a second equilibrium state will eventually be reached after a stepped disturbance is initiated in the test section. The computed Mach number change between the two equilibrium states could be obtained from equation (2):

$$\Delta M_c = \frac{5 \left(\frac{p_{t1}}{p_{s1}} \right)^{2/7}}{7M_1} \left[\frac{\Delta p_t}{p_{t1}} - \frac{\Delta p_s}{p_{s1}} \right] \quad (2)$$

where

$\Delta p_t \equiv p_{t2} - p_{t1}$ = total pressure change, psf

$\Delta p_s \equiv p_{s2} - p_{s1}$ = static pressure change, psf

Equation (2) is the linear approximation of equation (1) and is valid for small changes of pressure only. The validity of equation (2) is established by a comparison in table of the Mach number changes computed from equation (1) with those computed from equation (2). Small variations between these two changes are seen. Note that steady-state SEL data of p_t and p_s are used for the calculation. In other words, for one ambient pressure (1atm) and elevated temperature (120°F) flap-model test, a linear relationship between Mach number change and pressure changes exist for Mach number change up to ± 0.070 . The block diagram in figure 23 illustrates this cause-effect relationship. It is noted that the gains used in the three blocks of Figure 23 are different for different equilibrium conditions of the wind tunnel.

Table 2. Mach number changes.

Nominal Mach Number	Test Number	M ₁ (initial)	M ₂ (final)	$\Delta M = M_2 - M_1$	$\frac{\Delta M}{\Delta M} \times 100\%$
M = .8	2253	.8000	.7854	-.0146	-.0145
	2254	.7852	.8007	.0155	.0155
	2255	.8018	.7876	-.0142	-.0141
	2256	.7879	.8018	.0139	.0140
M = .95	1824	.9532	.9191	-.0341	-.0340
	1825	.9173	.9497	.0324	.0320
	1826	.9525	.9187	-.0338	-.0336
	1827	.9151	.9486	.0335	.0328
M = .95	2145	.9521	.9191	-.0330	-.0332
	2146	.9175	.9495	.0320	.0318
	2147	.9514	.9190	-.0324	-.0324
	2148	.9178	.9499	.0321	.0318
M = 1.05	1931	1.0530	.9802	-.0728	-.0728
	1932	.9762	1.0439	.0677	.0644
	1933	1.0536	.9802	-.0734	-.0733
	1934	.9759	1.0440	.0681	.0662
M = 1.2	2038	1.1966	1.1659	-.0307	-.0308
	2039	1.1652	1.1960	.0308	.0305
	2040	1.1974	1.1658	-.0316	-.0317
	2041	1.1657	1.1959	.0302	.0300

* State 2 has not reached equilibrium.

Relative Contributions of the Two Pressure Changes on the Mach Number Change

The two terms inside the brackets of equation (2) are percentage changes of total and static pressures. Experimental results of these two percentage changes are listed in table 3. The last column shows the ratio of percentage change of static pressure over the percentage change of stagnation pressure. The average ratio found is -6.4. If a new variable λ , defined as the ratio of these two percentage changes, is introduced, then equation (2) can be rewritten as:

$$\Delta M = - \frac{5 \left(\frac{p_{t1}}{p_{s1}} \right)^{2/7} \frac{\Delta p_s}{p_{s1}}}{7M_1} \left(1 - \frac{1}{\lambda} \right) \quad (3)$$

where

$$\lambda \equiv \left(\frac{\Delta p_s}{p_{s1}} \right) / \left(\frac{\Delta p_t}{p_{t1}} \right) = \left(\frac{p_{t1}}{p_{s1}} \right) \left(\frac{\Delta p_s}{\Delta p_t} \right) \quad (4)$$

The negative sign of λ indicates that the two pressure changes are opposite in directions; i.e., when one increases the other decreases and vice versa. The magnitude of λ shows that the test section Mach number change is dominated by the test chamber static pressure change. Therefore, equation (3) can be approximated as

$$\Delta M \approx - \frac{5 \left(\frac{p_{t1}}{p_{s1}} \right)^{2/7} \left(\frac{\Delta p_s}{p_{s1}} \right)}{7M_1} \quad (5)$$

Test Section Mach Number Response Speed

Equation (5) indicates that the test section Mach number change depends primarily on the change of static pressure. Since the latter possesses almost instantaneous response speed, fast response for Mach number can be expected. However, since the approximation given by equation (5) is valid only

Table 3. Pressure changes.

Nominal Mach Number	Test Number	P_s , static pressure, psf					P_t , total pressure, psf					Pressure Ratio λ
		P_{s1} (initial)	P_{s2} (final)	$\Delta P_s \equiv P_{s2} - P_{s1}$	$\frac{ \Delta P_s }{P_{s1}} \times 100\%$	P_{t1} (initial)	P_{t2} (final)	$\Delta P_t \equiv P_{t2} - P_{t1}$	$\frac{ \Delta P_t }{P_{t1}} \times 100\%$			
M = .80	2253	1391.2	1409.0	17.8	1.28	2120.8	2117.3	-3.5	.17	-7.5		
	2254	1409.8	1391.8	-18.0	1.28	2117.9	2122.9	5.0	.24		-5.3	
	2255	1391.3	1408.1	16.8	1.21	2124.2	2120.0	-4.2	.20		-6.1	
	2256	1408.0	1391.9	-16.1	1.14	2120.8	2125.7	4.9	.23		-5.0	
	1824	1183.5	1222.7	39.2	3.31	2122.5	2111.4	-11.1	.52		-6.4	
M = .95	1825	1225.5	1188.9	-36.6	2.99	2112.2	2123.5	11.3	.53	-5.6		
	1826	1183.7	1222.5	38.8	3.28	2121.5	2110.6	-10.9	.51	-6.4		
	1827	1223.8	1186.2	-37.6	3.07	2105.7	2116.8	11.1	.53	-5.8		
	2145	1183.2	1222.0	38.8	3.28	2120.7	2110.9	-9.8	.46	-7.1		
	2146	1224.9	1189.1	-35.8	2.92	2111.8	2123.8	12.0	.57	-5.1		
M = 1.05	2147	1184.1	1222.5	38.4	3.24	2120.0	2111.3	-8.7	.41	-7.9		
	2148	1226.4	1190.7	-35.7	2.91	2114.7	2127.2	12.5	.59	-4.9		
	1931	1051.1	1132.3	31.2	7.73	2118.6	2096.0	-22.6	1.07	-7.2		
	1932	1138.6	1064.9	-73.7	6.47	2096.7	2120.7	24.0	1.14	-5.7		
	1933	1051.2	1132.6	81.4	7.74	2120.3	2096.9	-23.4	1.10	-7.0		
M = 1.20	1934	1138.8	1064.8	-74.0	6.50	2096.6	2119.7	23.1	1.10	-5.9		
	2038	877.6	906.1	28.5	3.25	2118.5	2102.2	-16.3	.77	-4.2		
	2039	902.3	869.0	-33.3	3.69	2091.3	2097.5	6.2	.30	-12.3		
	2040	876.4	908.4	32.0	3.65	2117.7	2107.5	-10.2	.48	-7.6		
	2041	908.8	878.5	-30.3	3.33	2108.1	2118.9	10.8	.51	-6.5		

for $\frac{\lambda}{\lambda - 1}$ or 86 percent of the total Mach number change, it implies that once the test section is disturbed, the test section Mach number will be changed almost instantaneously to within 86 percent of its total change. The final 14 percent change of test section Mach number then will be dictated by the large time constant (6 to 8 seconds) of the total pressure change Δp_t as given by equation (2) or (3). The dynamic relationship between the drag force change ΔD in the test section and the resulting Mach change ΔM can be described by the block diagram shown in figure 24.

It should be noted that gain K in the first block of figure 23 has the units of psf/lb_f and assumes different values for different equilibrium conditions of the test section. Experimental values of K were found at .0168, .0313, .0617, and 0.143 for nominal Mach numbers of .80, .95, 1.05, and 1.20, respectively.

Dynamic Model of the Flow Process

The dynamic relationship between the pressures in the test section and in the big end has been constructed as

$$\frac{\Delta p_t (\Delta s)}{\Delta p_s (\Delta s)} = \frac{K'}{1 + \tau s} \quad (6)$$

where K' is the gain and τ is the time constant. This first-order transfer function was actually used in calculating the time constants of the flow process which are tabulated in table 1.

For the oscillation tests, Δp_s is a square wave input (see fig. 16) which can be expressed as

$$\Delta p_s = u(t) - u(t - a) + u(t - 2a) - u(t - 3a) \dots \quad (7)$$

where $u(t)$ is the unit step function, $u(t-a)$ is the delayed unit step function and the delay a is one half of the period of the input square wave.

The solution of equation (6) for this square wave input is

$$\Delta p_t = K'(1 - e^{-t/\tau}) u(t) - K'(1 - e^{-(t-a)/\tau}) u(t - 2a) \quad (8)$$

$$K'(1 - e^{-(t-2a)/\tau}) u(t - 3a) + K' a_0 e^{-t/\tau} \dots$$

where a_0 is the initial value of Δp_t .

Figure 25 illustrates the wave form of the total pressure as calculated from equation (8) with $a = 5$ sec. It matches closely the response of transducer 101T shown in figure 15 where it is shown that an initial transient period is required before the sawtooth steady-state response is fully developed. The sawtooth steady-state response can be shown as

$$\Delta p_{t_{ss}} = K' \left[1 - \frac{e^{-t/\tau}}{1 + e^{-a/\tau}} \right] \quad (9)$$

during the half period when the step is applied (i.e., when the flap is opened)

and

$$\Delta p_{t_{ss}} = K' \left[\frac{e^{-(t-a)/\tau}}{1 + e^{-a/\tau}} \right] \quad (10)$$

during the next half period when the step is removed (i.e., when the flap is closed).

The maximum and minimum total pressure at steady-state then can be calculated from equations (9) and (10) respectively as

$$\Delta p_t \text{ max} = \frac{K'}{1 + e^{-a/\tau}} < K' \quad (11)$$

$$\Delta p_t \text{ min} = \frac{K'}{1 + e^{a/\tau}} > 0 \quad (12)$$

The peak-to-peak steady-state total pressure becomes

$$\Delta p_t \text{ max} - \Delta p_t \text{ min} = K' \tanh (a/2\tau) < K' \quad (13)$$

It should be pointed out that equation (11) indicated that the maximum total pressure at steady-state is less than K' , which would be one steady-state response if the input were a single-step function. The response of total pressure for a single-step static input is also shown in figure 25.

Based on equations (11), (12), and (13) and using responses from transducer 101, process time constant τ was computed. The results are included in table 1. It is noticed that quantitative agreements are not very good between the values computed by this approach and those computed directly.

CONCLUDING REMARKS AND RECOMMENDATIONS

This report includes the presentation and analysis of data obtained during a series of tests at the NASA-Langley eight-foot transient pressure tunnel. The tests were only partially successful due to the over-sized pressure transducers selected. The incorrect selection of pressure transducers was caused by the unexpected small pressure variations when the tunnel was perturbed by the flap motion. Consequently, only a limited amount of data are intelligible and could be used for analysis. However, several significant findings were observed and are summarized in the following:

1. Transport lag - insignificant as compared to the time constant of the flow process even if it exists;
2. Test section static pressure - rapidly changing even though the total pressure in the test section is slowly varying;
3. Total pressure - slowly varying first-order type response with time constants varying between 4 to 9 seconds; total pressure changes at various sites approximately identical;
4. $\Delta p_s / \Delta p_t \gg 1$ - there exists a fixed ratio between the changes of the static and total pressures in the test section;
5. Mach number - the test section Mach number change is dominated by the static pressure change in the test section; the test section Mach number change is a linear function of the static and total pressure changes in the test section.

The following requirements on instrumentation were also observed based on experimental evidence:

1. Together with equation (2) and data in tables 2 and 3, it is possible to calculate the two pressure changes for small Mach number variations. Table 4 lists these pressure changes for Mach number changes of .002 at different operating conditions. This implies that the total pressure measurement device must be sensitive to the fraction of one psf in order to control the test section Mach number with an accuracy of .002.

2. If the test section Mach number is the desirable Mach number to be controlled, then either the probe of the pressure measuring device should be located inside the test section or some prediction technique should be applied to the pressure measurements made outside the test section. As indicated in figure 10, the SEL system and the ideal manometer with its probe located in the plenum are not capable of following the rapid static pressure change in the test section. It is fairly safe to assume that this is due to the combination of the dynamics of the plenum filling or emptying process and the dynamics of the manometer.

In summary, it can be said the test did provide a certain amount of useful information about the flow process of the wind tunnel which has not been reported before. It is also believed that better instrumentation in a future test of this kind will provide more quantitative as well as qualitative data for substantiating the modeling effort of NTF.

Table 4. Pressure variations for Mach number variations of .002.

Nominal Mach Number	p_s , static pressure		p_t , stagnation pressure	
	$ \Delta p_s $	$\frac{ \Delta p_s }{p_{s1}} \times 100\%$	$ \Delta p_t $	$\frac{ \Delta p_t }{p_{t1}} \times 100\%$
M = .80	2.37	.17	.60	.028
M = .95	2.30	.19	.67	.052
M = 1.05	2.21	.20	.66	.031
M = 1.20	2.01	.23	.71	.034

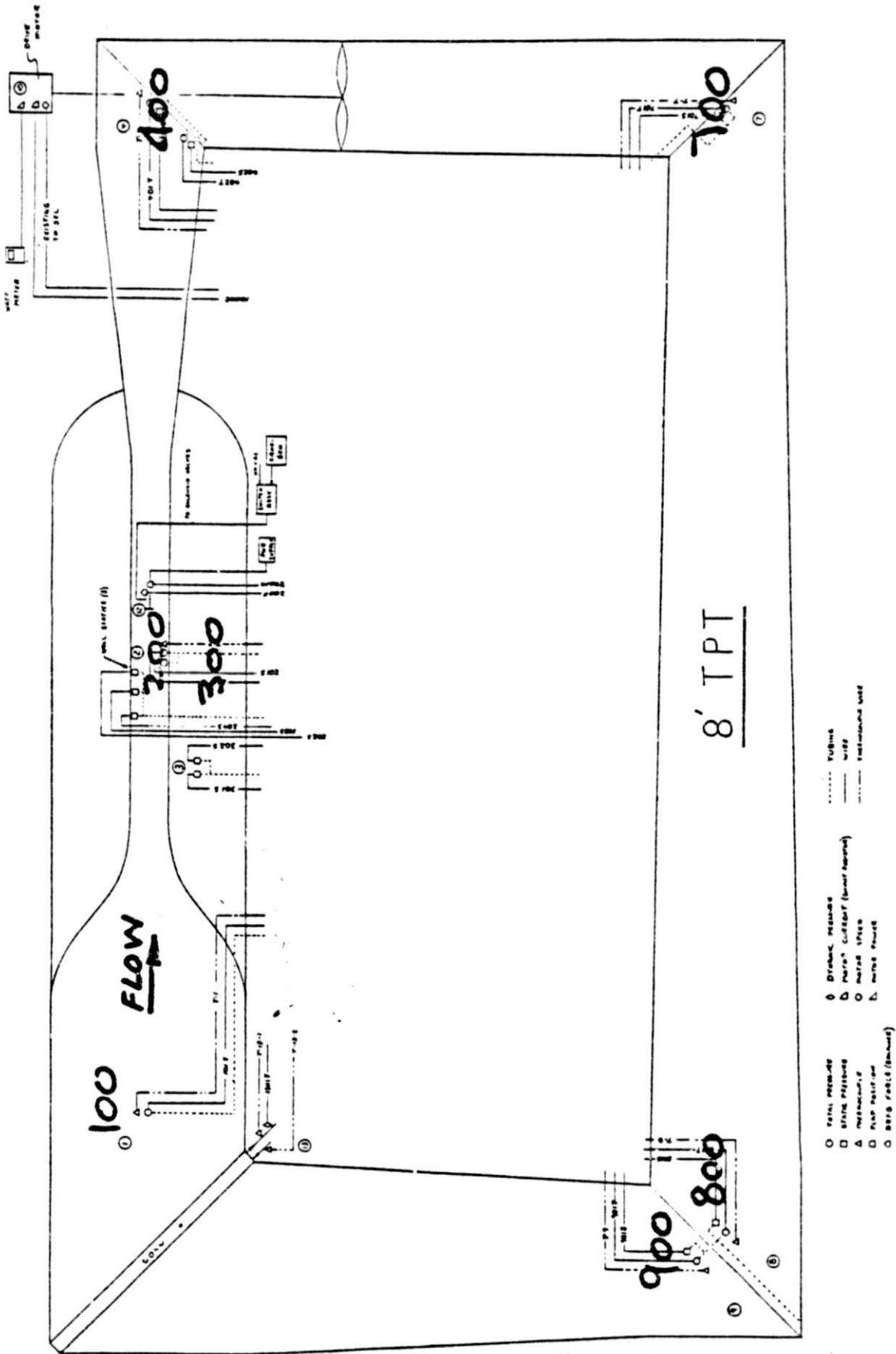


Figure 1. Instrumentation schematic.

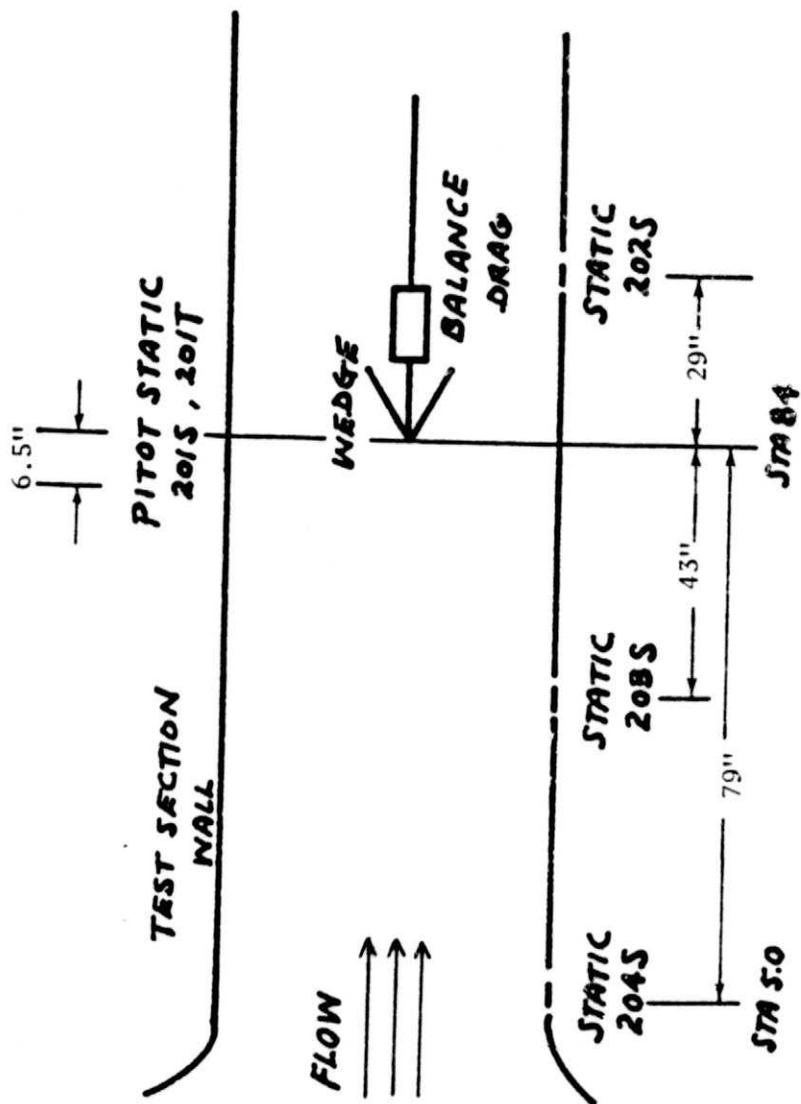


Figure 2. Test section instrumentation.

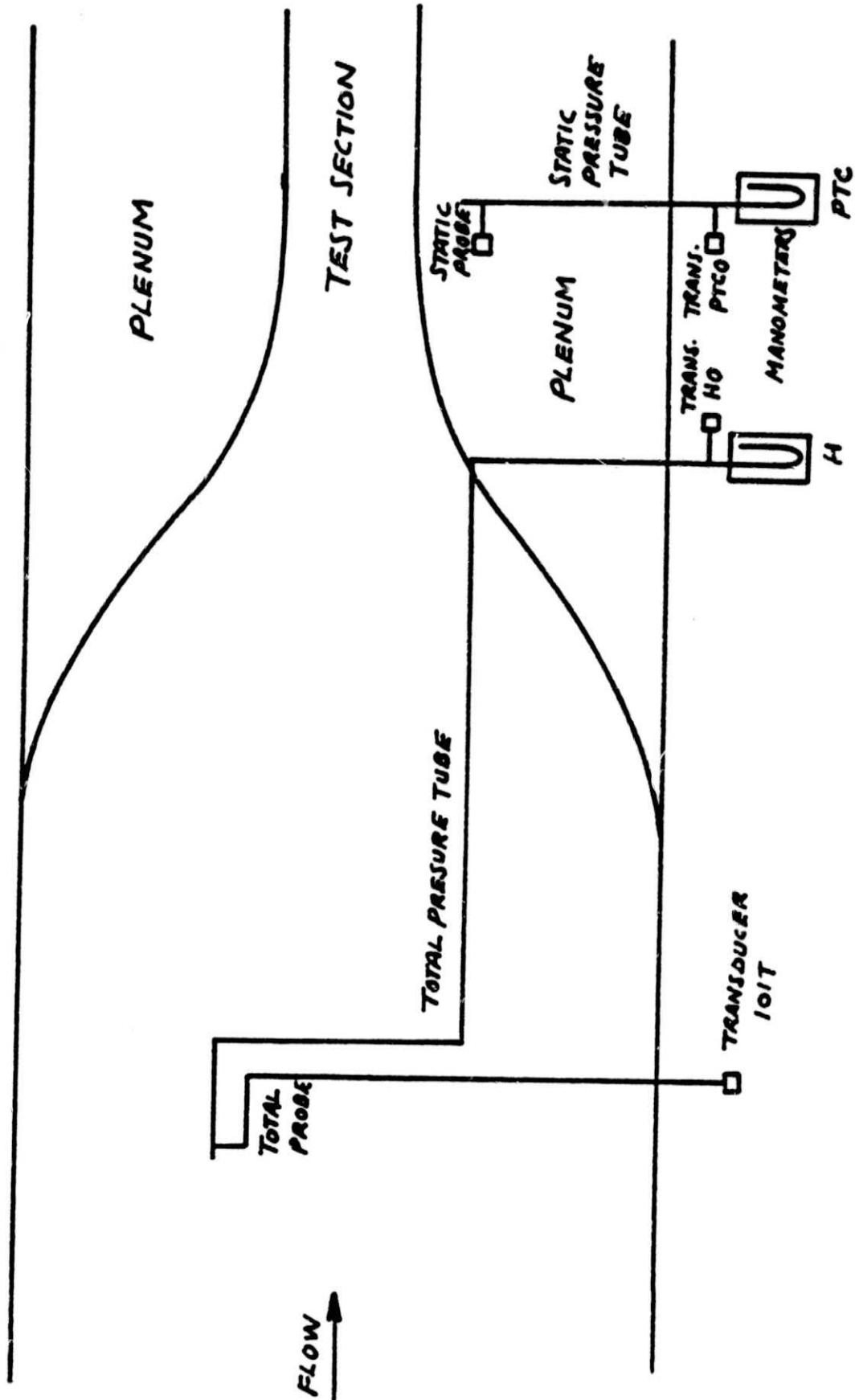


Figure 3. Manometer locations.

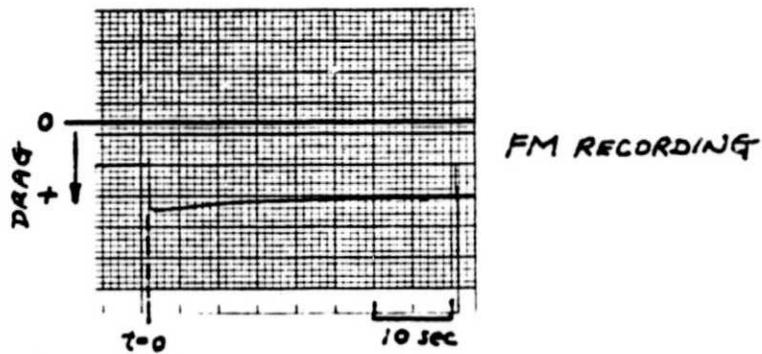
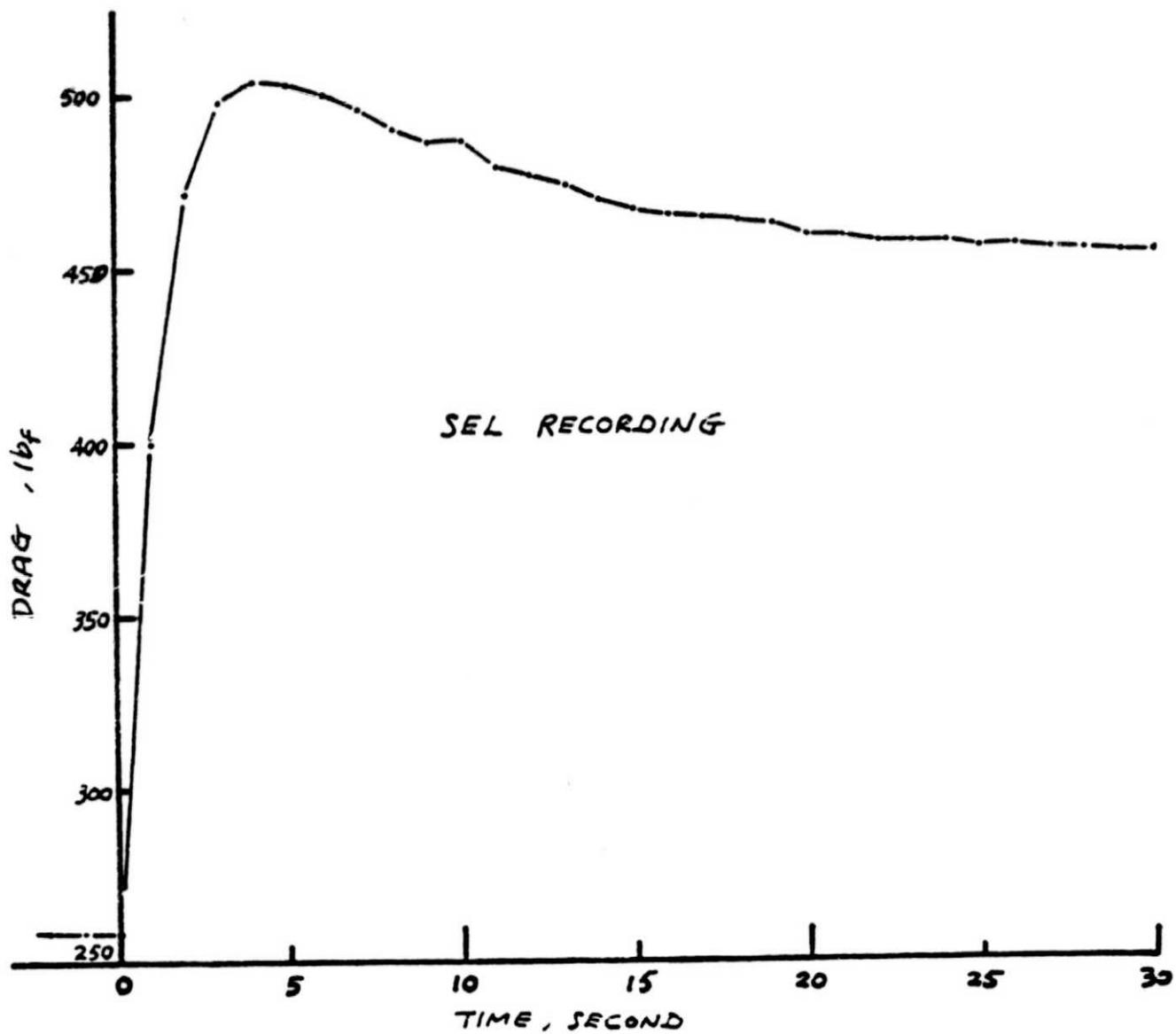


Figure 4. Drag (run 19.31).

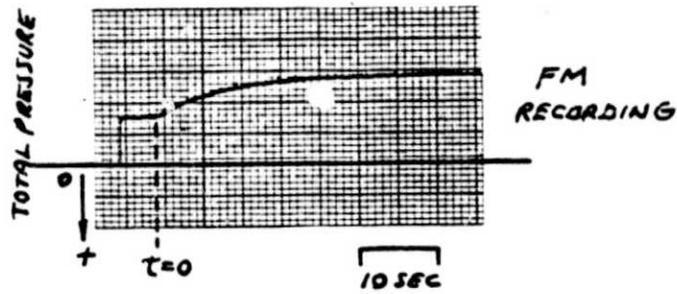
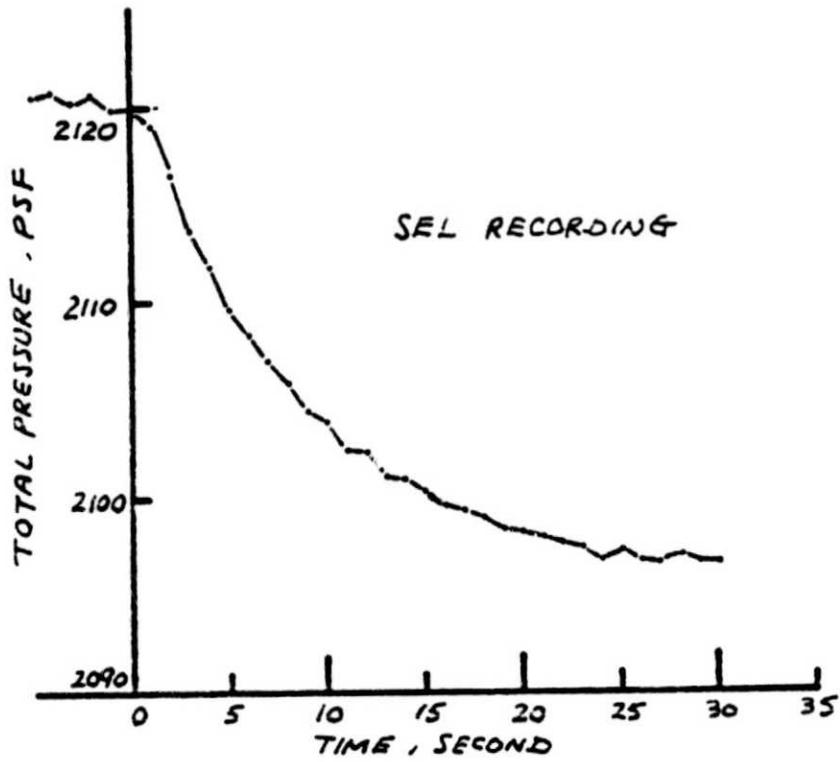


Figure 5.. 101T (run 19.31).

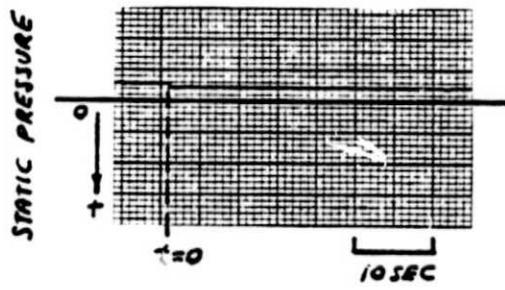


Figure 6. 201S (run 19.31).

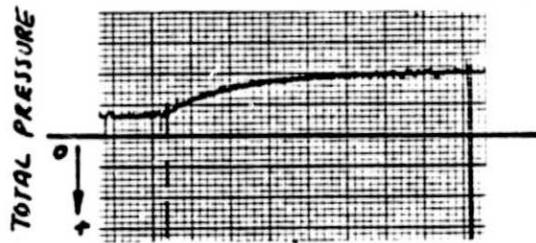


Figure 7. 201T (run 19.31).

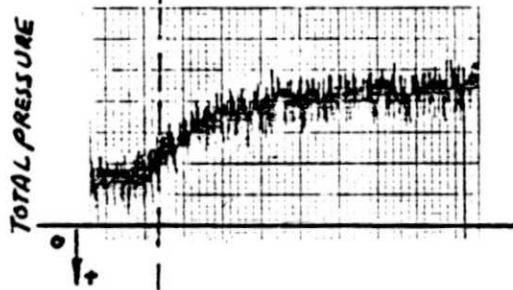


Figure 8. 701T (run 19.31).

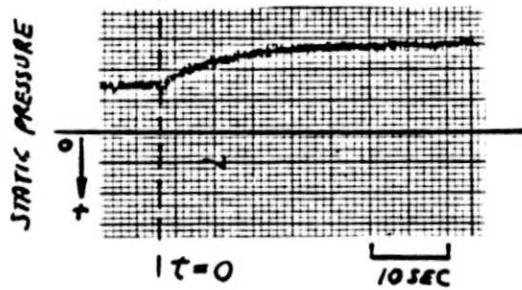


Figure 9. 701S (run 19.31).

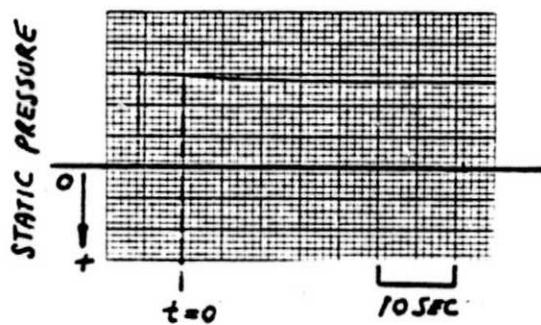
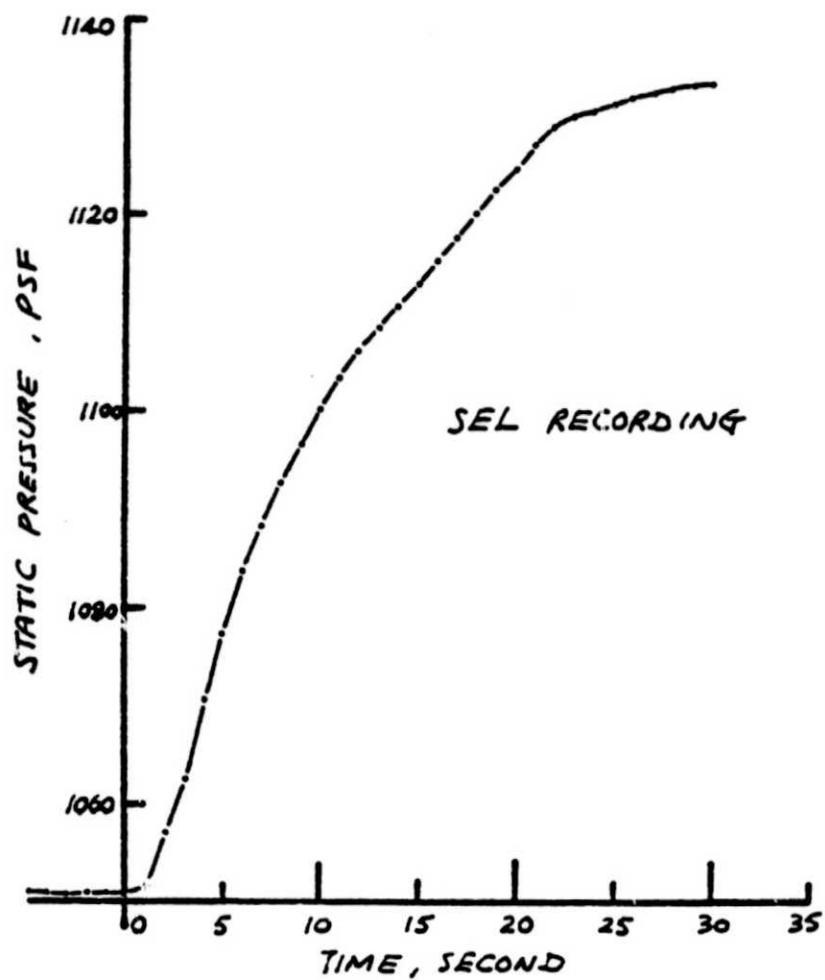


Figure 10. 302S (run 19.31).

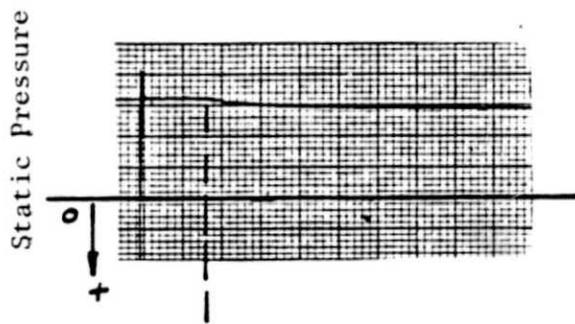


Figure 11. 203S (run 19.31).

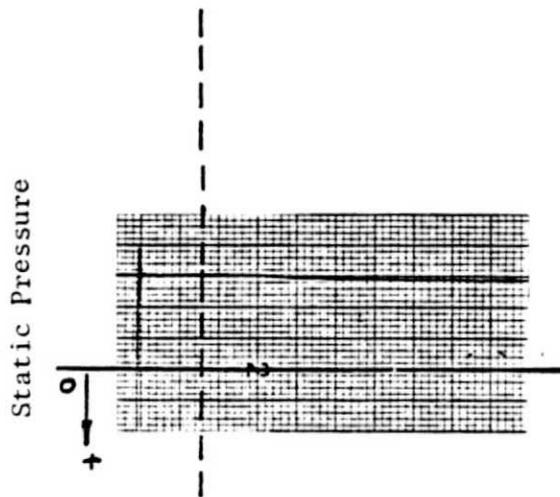


Figure 12. 204S (run 19.31).

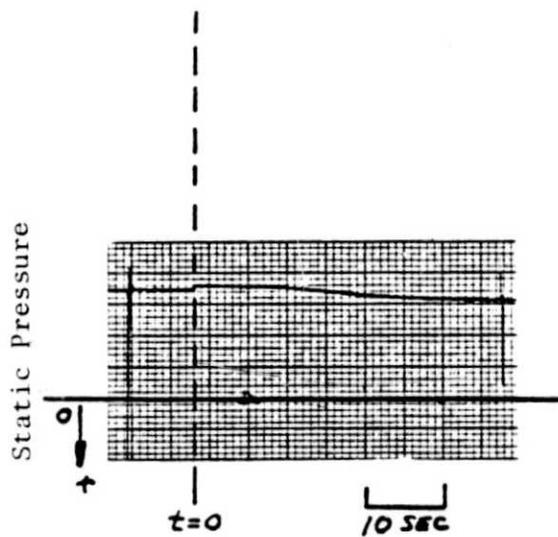


Figure 13. 202S (run 19.31).



Figure 14. Drag (run 19.35).

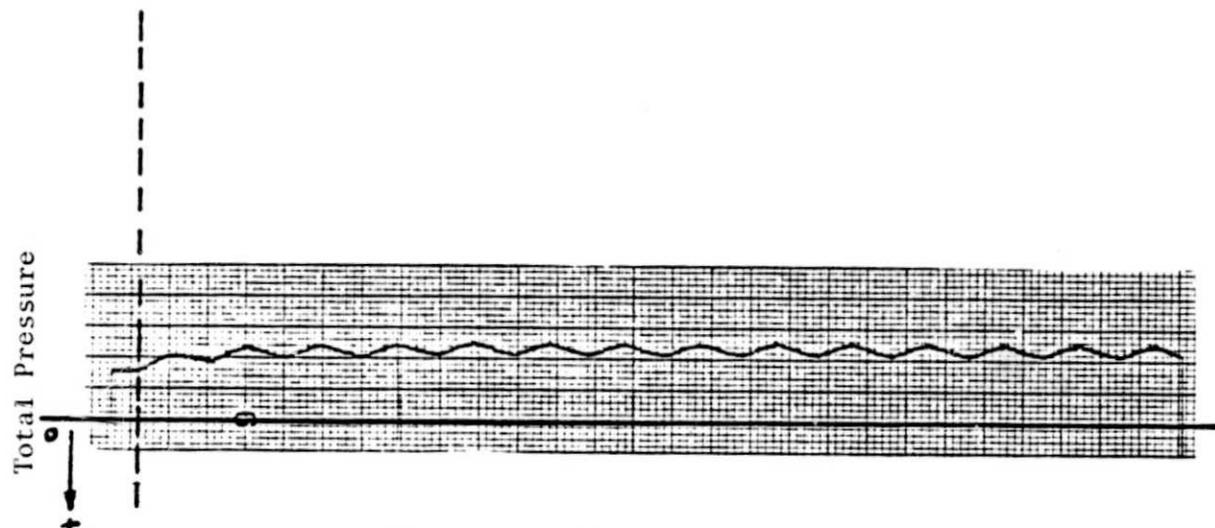


Figure 15. 101T (run 19.35).

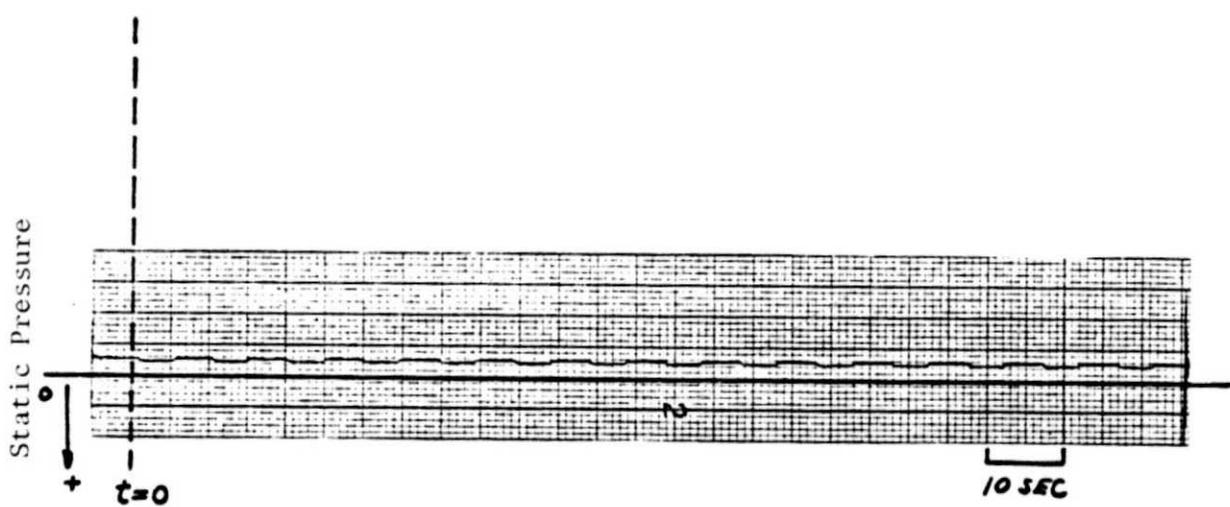


Figure 16. 201S (run 19.35).

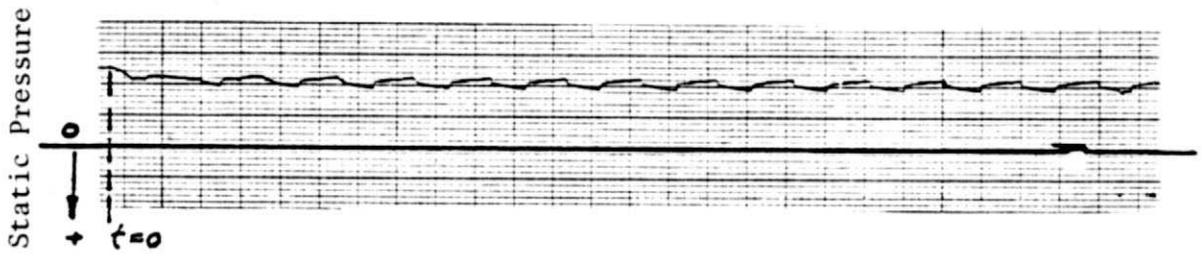


Figure 17. 203S (run 19.35).

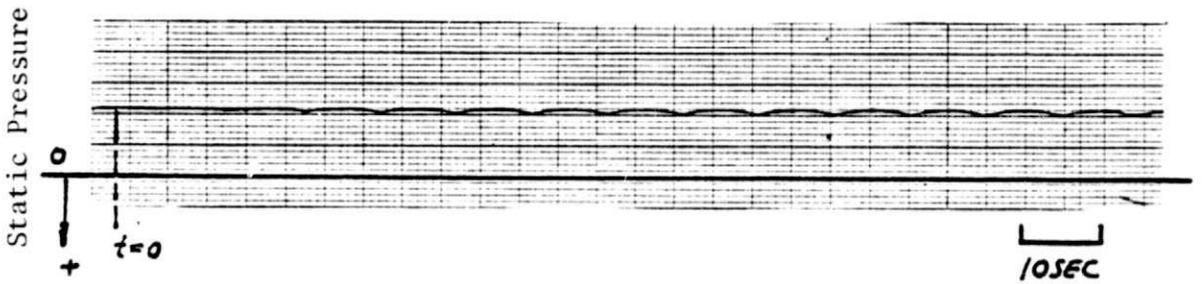


Figure 18. 204S (run 19.35).

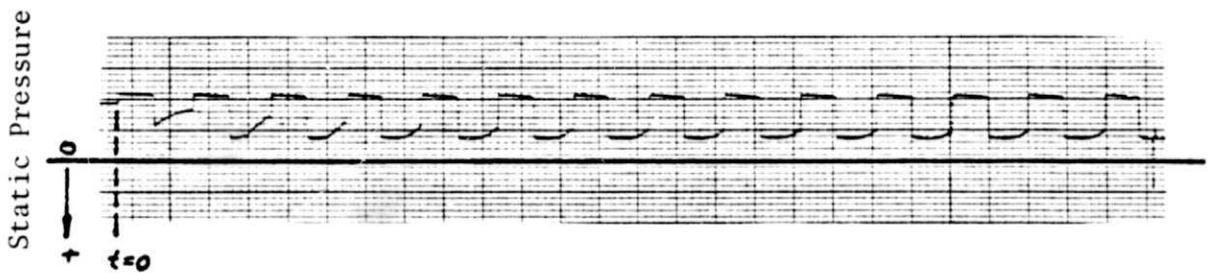


Figure 19. 202S (run 19.35).

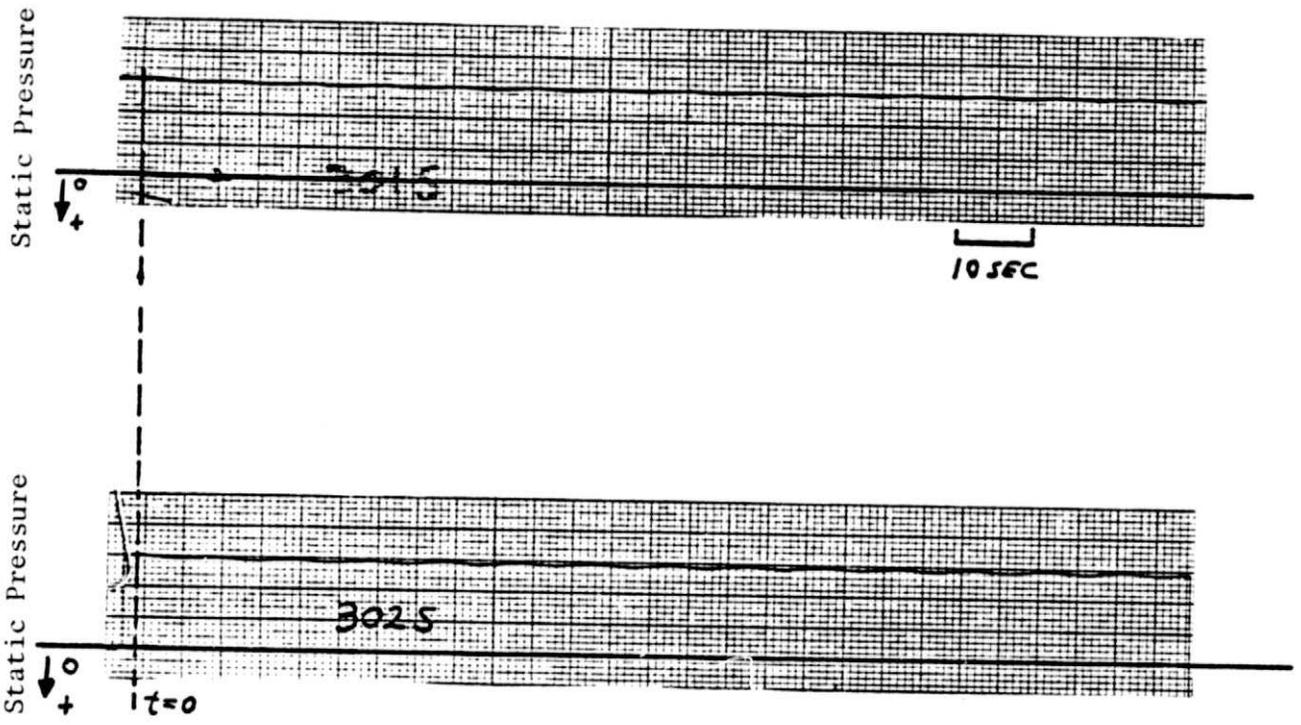


Figure 20. 301S and 302S (run 19.35)

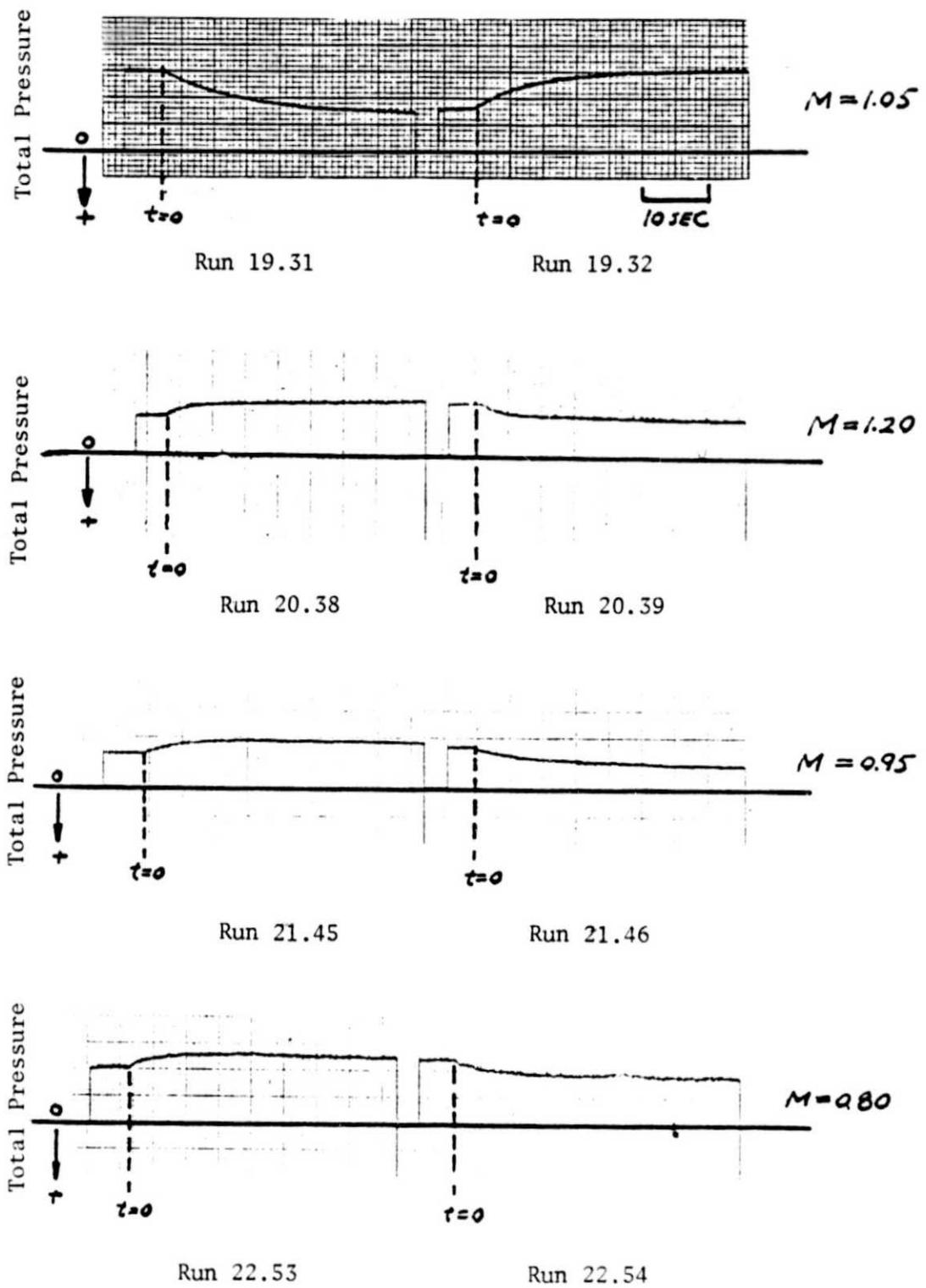


Figure 21. 101T.

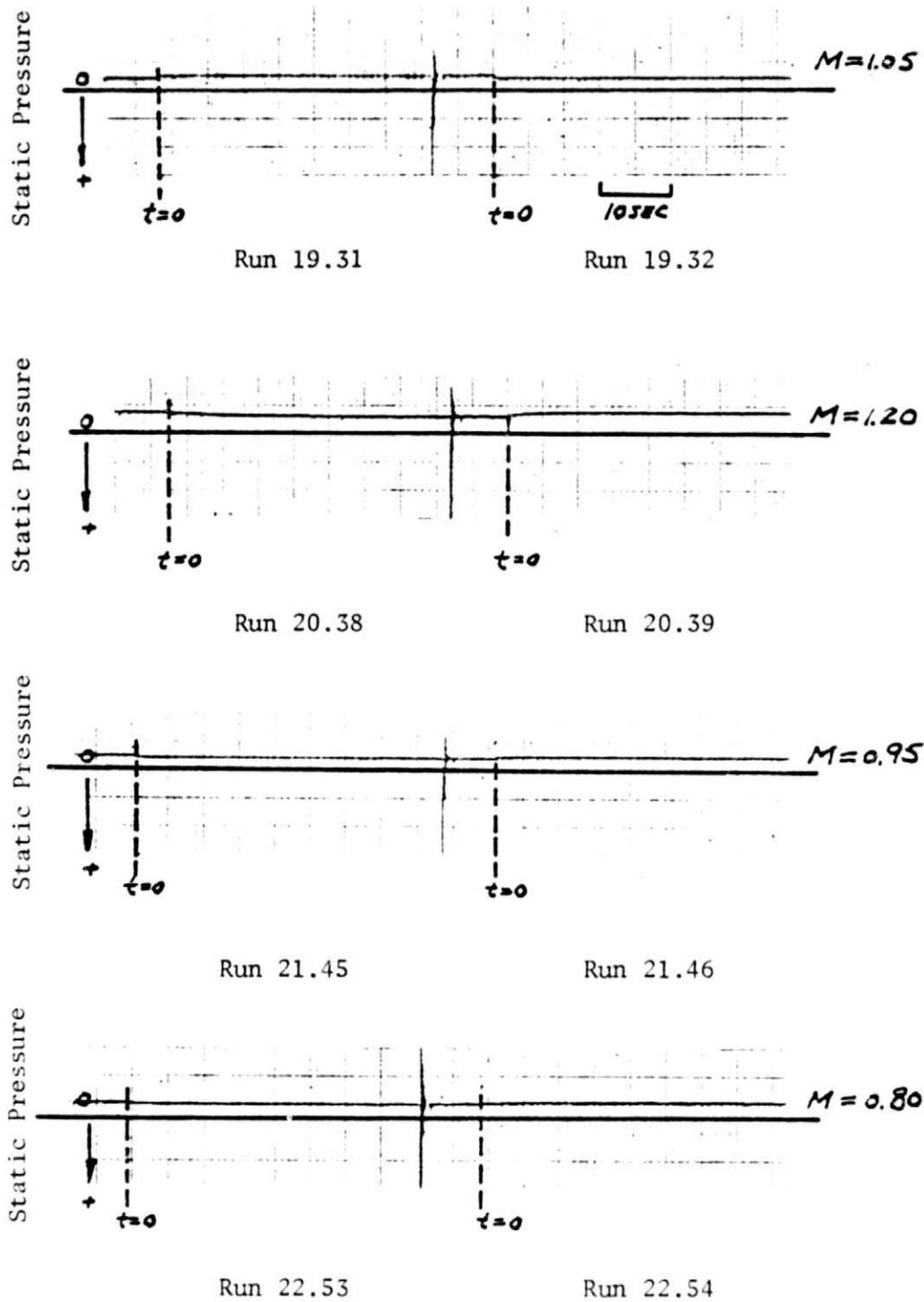


Figure 22. 201S

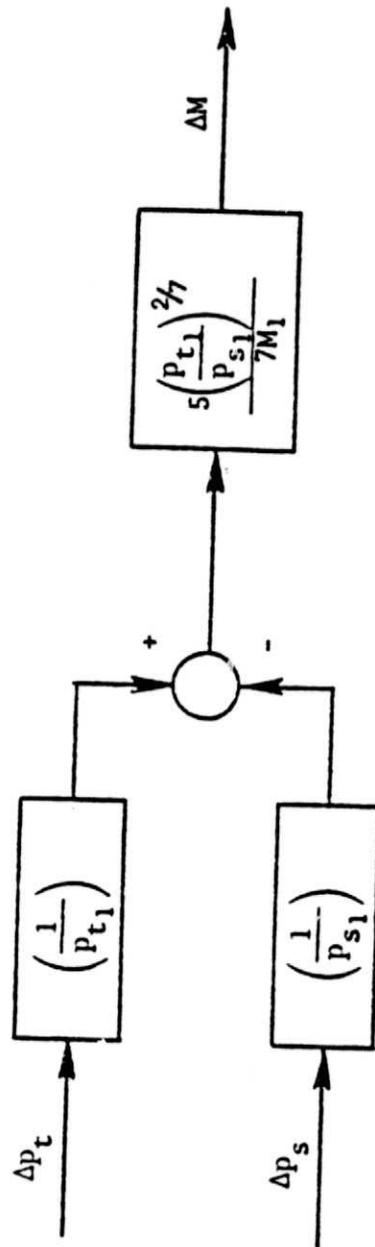


Figure 23. Linear (static) relationship between Mach number change and pressure changes.

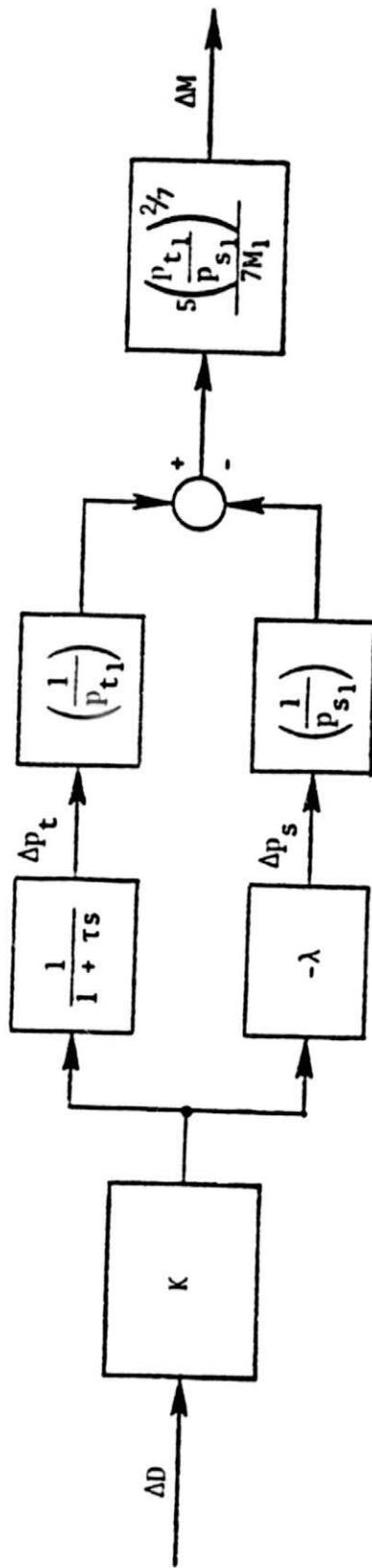


Figure 24. Dynamic relationship between Mach number change and Drag change.

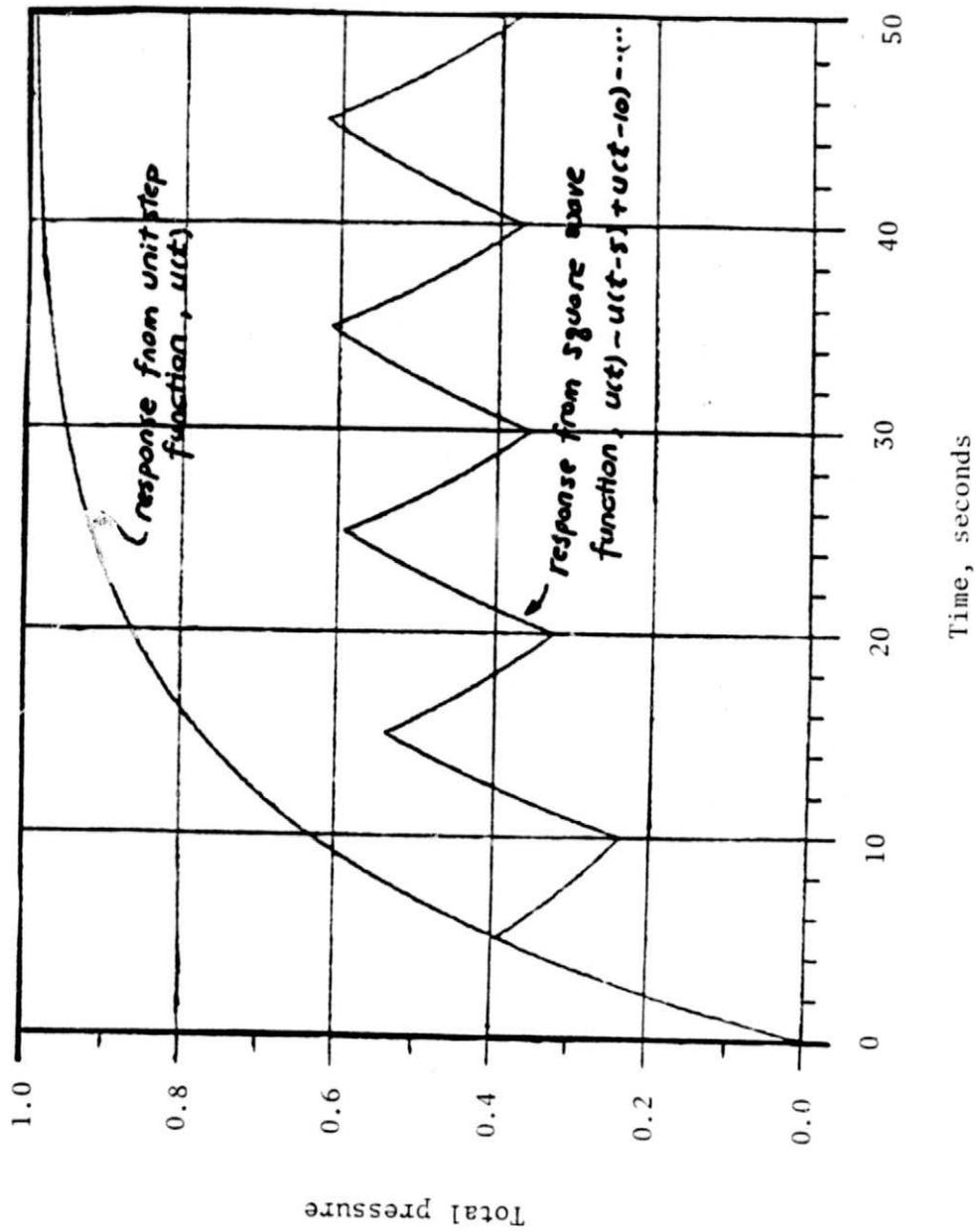


Figure 25. Simulated total pressure changes.